HIV-1 Tat protein promotes neuronal dysregulation by inhibiting E2F transcription factor 3 (E2F3)

Received for publication, April 27, 2018, and in revised form, December 17, 2018 Published, Papers in Press, December 27, 2018, DOI 10.1074/jbc.RA118.003744

Maryline Santerre[‡1], Asen Bagashev[‡§1,2], Laura Gorecki[‡], Kyle Z. Lysek[‡], Ying Wang[‡], Jenny Shrestha[‡], Fabiola Del Carpio-Cano[‡], Ruma Mukerjee[‡], and Bassel E. Sawaya[‡§¶3]

From the [‡]Molecular Studies of Neurodegenerative Diseases Laboratory, FELS Institute for Cancer Research and Molecular Biology, the [§]Department of Anatomy and Cell Biology, and the [¶]Department of Neurology, Temple University School of Medicine, Philadelphia, Pennsylvania 19140

Edited by Paul E. Fraser

Individuals who are infected with HIV-1 accumulate damage to cells and tissues (*e.g.* neurons) that are not directly infected by the virus. These include changes known as HIV-associated neurodegenerative disorder (HAND), leading to the loss of neuronal functions, including synaptic long-term potentiation (LTP). Several mechanisms have been proposed for HAND, including direct effects of viral proteins such as the Tat protein. Searching for the mechanisms involved, we found here that HIV-1 Tat inhibits E2F transcription factor 3 (E2F3), CAMP-responsive element–binding protein (CREB), and brain-derived neurotropic factor (BDNF) by up-regulating the microRNA miR-34a. These changes rendered murine neurons dysfunctional by promoting neurite retraction, and we also demonstrate that E2F3 is a specific target of miR-34a. Interestingly, bioinformatics analysis revealed the presence of an E2F3-binding site within the *CREB* promoter, which we validated with ChIP and transient transfection assays. Of note, luciferase reporter assays revealed that E2F3 up-regulates *CREB* expression and that Tat interferes with this up-regulation. Further, we show that miR-34a inhibition or E2F3 overexpression neutralizes Tat's effects and restores normal distribution of the synaptic protein synaptophysin, confirming that Tat alters these factors, leading to neurite retraction inhibition. Our results suggest that E2F3 is a key player in neuronal functions and may represent a good target for preventing the development of HAND.

One of the major issues associated with HIV-1 brain invasion is the increased incidence of neurite retraction (1, 2). This event was observed even in the presence of combination antiretroviral therapies. Neurite retraction is the result of secondary complications such as HIV-associated dementia, mild neurocognitive disorder, and asymptomatic neurocognitive impermanent, with HIV-associated dementia being the most severe and asymptomatic neurocognitive impermanent being asymptomatic but with pronounced physiological changes in the central nervous system (3).

The exact molecular mechanisms leading to neurite retraction are not fully understood. Several reports indicated that HIV-infected macrophages and microglia produce neurotoxins (*e.g.* viral proteins) that have the ability to cause neuronal deregulation. Tat is among the released viral proteins that have been considered to be deleterious to neurons; however, the mechanisms used by Tat to cause neurodegeneration remain unclear (4, 5).

The transactivator regulatory (Tat) protein has been implicated in the pathophysiology of the neurocognitive deficits associated with HIV infection (6). This is the earliest protein to be produced by the proviral DNA in the infected cell. The protein not only drives the regulatory regions of the virus but may also be actively released from infected astrocytes and microglia cells and interacts with the cell surface receptors of neighboring uninfected neuronal cells in the brain, leading to cellular dysfunction. It may also be taken up by these cells (7, 8) and can activate a number of host genes (9, 10). Additionally, Tat production is not impacted by the use of antiretroviral drugs once the proviral DNA has been integrated within the host cell genome. In adult animals, Tat affects pre-attentive processes and spatial memory. Tat-transgenic model are marked by glial cell activation and neuronal loss (11). In animals, Tat causes loss of selective populations of neurons *in vitro* and *in vivo* (12). Regions particularly susceptible to Tat neurotoxicity include the striatum, the dentate gyrus, and the CA3 region of the hippocampus (13, 14). Further, neuropathological studies from patients with HIV infection show a preferential loss of neurons in the dentate gyrus and striatum (15). Tat also depolarizes the neuronal cell membrane when applied extracellularly to outside-out membrane patches providing strong evidence for direct excitation of neurons on the cell surface.

Tat induces dramatic increases in levels of intracellular Ca^{2+} in neurons followed by mitochondrial Ca^{2+} uptake, generation of ROS, activation of caspases, and eventually neuronal deregulation. These include alteration of synaptic plasticity and suppression of long-term potentiation (LTP),[4] leading to premature brain aging.

This work was supported by National Institutes of Health Grants R01-NS059327, R01-NS076402, R01-MH093331, and R01-AG054411 (to B. E. S.). The authors declare that they have no conflicts of interest with the contents of this article. The content is solely the responsibility of the authors and does not necessarily represent the official views of the National Institutes of Health.

[1] Both authors contributed equally to this work.

[2] Present address: Dept. of Cancer Pathobiology, Children's Hospital of Philadelphia, 4300 Colket Translational Research Bldg., 3501 Civic Center Blvd., Philadelphia, PA 19104.

[3] To whom correspondence should be addressed: Fels Institute for Cancer Research, Lewis Katz School of Medicine, Temple University, 3307 N. Broad St., Philadelphia, PA 19140. Tel.: 215-707-5446; Fax: 215-707-5948; E-mail: sawaya@temple.edu.

[4] The abbreviations used are: LTP, long-term potentiation; CREB, CAMP-responsive element–binding protein; BDNF, brain-derived neurotropic factor; ANOVA, analysis of variance; RFP, red fluorescent protein; qPCR, quantitative PCR; HIVE, HIV-1–infected patient with signs of encephalitis; H3K9, histone H3 Lys-9; DMEM, Dulbecco's modified Eagle's medium; GAPDH, glyceraldehyde-3-phosphate dehydrogenase; MOI, multiplicity of infection; DAPI, 4′,6-diamidino-2-phenylindole; Luc, luciferase.

The exact molecular mechanisms used by Tat to perform these functions are not well understood and remain to be studied.

We recently demonstrated that neuronal deregulation in Tat-treated cells is microRNA-dependent (5). Using human neuron cells, we showed that Tat up-regulates the expression of miR-34a and down-regulates the expression levels of CREB and brain-derived neurotropic factor (BDNF) proteins; both factors play a key role in LTP (16, 17). In this regard, it has been shown that the expression pattern of BDNF, a direct transcriptional target of CREB, has been altered not only in HIV mouse model and HIV-associated neurodegenerative disorder (HAND) human brain sections postmortem, but in other neurological paradigms as well, which shows the fundamental significance of this pathway in neuronal cell survival and LTP (18). Intriguingly, neither protein (CREB or BDNF) is a direct target of miR-34a, which points to the existence of an intermediate transcription factor that is under the direct regulation of miRNA-34a and is a positive regulator of CREB. This could also mean that Tat decreases expression levels of these two proteins through an alternative mechanism that yet remains to be determined.

Here, we showed that Tat is using miR-34a and its downstream target E2F3 to inhibit CREB and BDNF protein functions. We also demonstrated, for the first time, that E2F3 protein is a positive regulator of the *CREB* promoter. Remarkably, this functional interplay between Tat, miR-34a, and E2F3 was enough to cause alteration of synaptophysin distribution, leading to neurite retraction and eventually to LTP inhibition.

Results

HIV-1 Tat protein has been shown to be associated with neuronal dysfunction; however, the exact mechanisms involved are not fully understood. In this regard, we previously demonstrated the ability of Tat to induce changes in miRNA expression in neuronal cells leading to the deregulation of expression levels of several cell factors implicated in LTP and long-term depression, such as CREB and BDNF. Here, we aimed to decipher the mechanisms leading to neurite retraction by focusing on the CREB-BDNF pathway.

HIV-Tat protein induces neurite retraction

First, we assessed the effect of extracellular Tat on intracellular calcium secretion. Human neuronal cells, SH-SY5Y (1×10^5), grown in serum-free medium, were treated with 10 nM (final concentration) recombinant Tat protein for 30 min. The cells were incubated with Fluo-3, and intracellular calcium was measured every 3 s using confocal microscopy (Fig. 1*A*). Within seconds, Tat addition led to a dramatic increase of intracellular calcium [Ca^{2+}]. A montage of calcium increase is displayed in Fig. 1*B*.

It has been shown that calcium is involved in many intracellular and extracellular process such as synaptic plasticity and cell-to-cell communication (19). Further, calcium channel antagonists have been shown to play a role in preventing neuronal damage (20, 21). Therefore, we examined whether Tat-induced [Ca^{2+}] can lead to neurite damage. We recorded in a live cell setting the ability of the cells to branch out and to communicate with other neurons. This was followed by measurements of the actual surface area covered by SH-SY5Y cells that were seeded in duplicate (mock untreated or treated with Tat) in ~40% confluences in differentiating medium. The cells were monitored for 20 h prior to the addition of 10 ng/ml recombinant Tat protein and then monitored for an additional 12 h. Automatic bright field contrast–snap shot images were taken every 30 min to evaluate the status of neurite outgrowth progression. As shown in Fig. 1*C*, measurement of the covered area revealed that the addition of Tat resulted in neurite retraction and a decrease of the covered area that lasted until the 32nd hour followed by a modest recovery when compared with the mock untreated.

Similarly, using primary mouse neurons isolated from the hippocampal area of embryonic day 18 pups, we showed that the addition of Tat protein led to neurite retraction when compared with the mock untreated neurons (Fig. 1*D*). The experiments in *C* and *D* were repeated three times each, and the results were analyzed using an ANOVA test ($p < 0.05$ and 0.001, respectively).

These results provided the rationale to examine the functional impact of this deregulation on neurite stability. It has been shown that synaptogenesis and the stability of synapses are key players for proper neuronal function, signal transfer and LTP (22). Therefore, we attempt to visualize and quantify the synaptic formation. Using the Cell Light transduction system (Life Technologies, Inc.), we transduced an RFP-tagged synaptophysin (MOI 5) into primary mouse neurons (mock and/or treated with Tat). Synaptophysin visualization is used as a marker for synaptic structures (23). As shown in Fig. 2*A*, there were significantly fewer synaptophysin puncta (*red*), corresponding to synaptic endings, in Tat-treated mouse neurons compared with mock treatment. Nuclei were stained with DAPI (*blue*). Additionally, a clear and obvious morphological change was observed in cells treated with Tat when compared with the mock untreated. Quantification of the positive puncta revealed a significant decrease at 24 h after Tat treatment (Fig. 2*B*) without affecting the size of the synaptic vesicles (Fig. 1*C*).

To further confirm this observation, we examined the status of Reelin protein (RELN) in Tat-treated cells. Reelin is a protein that regulates dendrite growth and controls cell-to-cell interactions during development (24). In adult brain, Reelin modulates synaptic plasticity by enhancing the induction of the LTP (25). Reelin loss or inhibition was shown to be associated with other diseases, such as schizophrenia (26). Therefore, we measured the expression of Reelin in Tat-treated SH-SY5Y cells. Twenty-four hours post-treatment, RNA was collected and subjected to quantitative PCR (qPCR). As shown in Fig. 2*D*, the addition of Tat decreases the level of Reelin by almost 50% when compared with the mock untreated. These results confirmed our observation and hypothesis regarding the ability of Tat to cause neurite retraction.

HIV-1 Tat down-regulates expression levels of CREB and BDNF

Neurite elongation is normally associated with activation and accumulation of the cytoskeleton component tubulin, and neurotropic factors, such as BDNF protein (27). Further, it has been shown that neuronal development and regulation of LTP and LDP depend on the functions of several transcription fac-

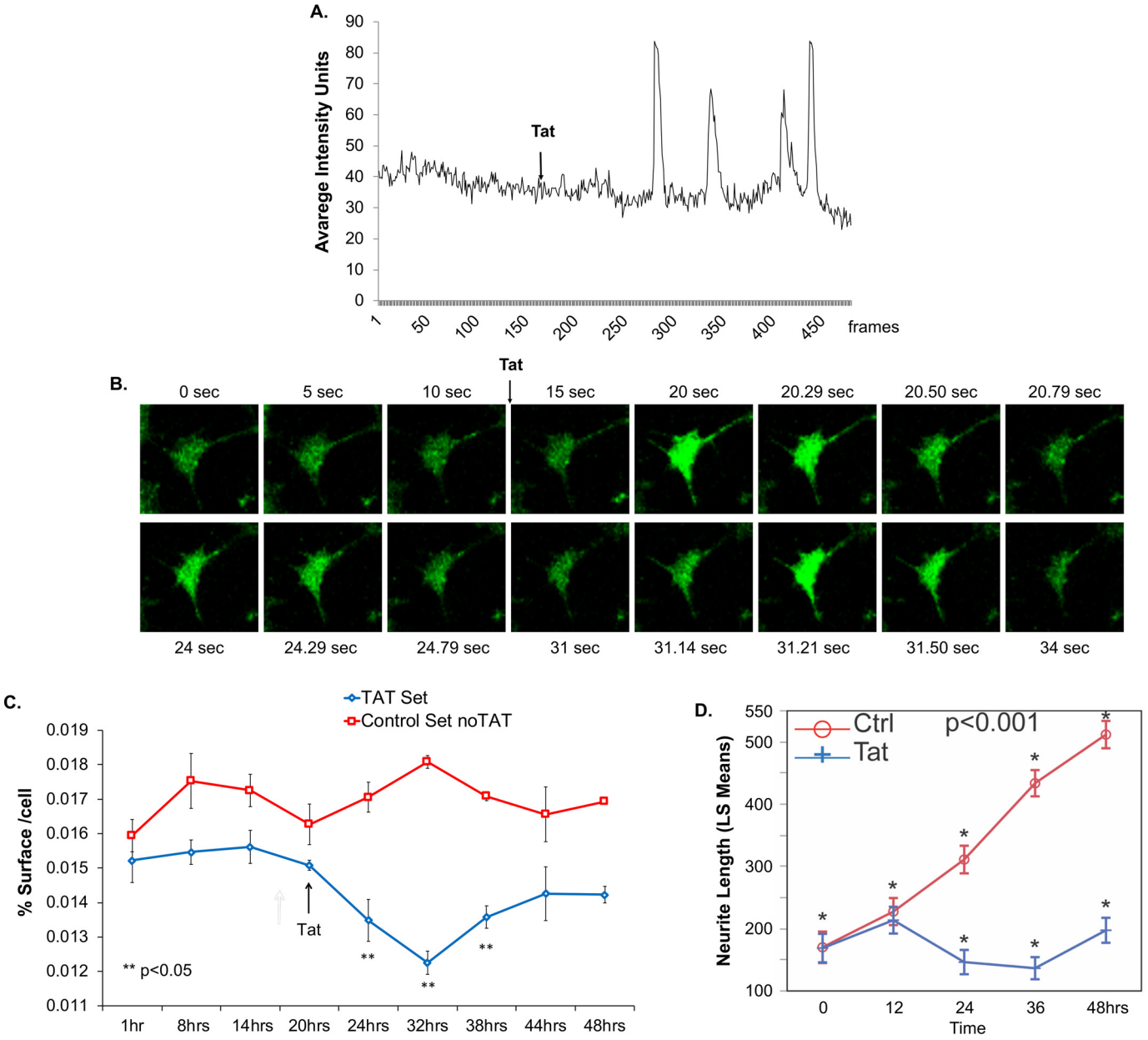

Figure 1. Tat promotes neurite retraction. *A*, calcium levels in Tat-treated neurons. SH-SY5Y cells were incubated with Fluo-3 (Molecular Probes, Inc.), and intracellular calcium (*green*) was measured every 3 s using confocal microscopy. *B*, montage of images collected from cells at different time points. All measurements were performed using $n = 100$, and the results are statistically significant using Student's *t* test ($p < 0.05$). *C*, SH-SY5Y cells were seeded at 40% confluence in 6-well plates with 10 μM retinoic acid medium. *D*, neurite lengths were measured in primary mouse neurons isolated from the hippocampal area of embryonic day 18 pups treated with Tat protein. Plates in *C* and *D* were placed on a live cell imaging station, and bright field contrast images from the same field were acquired every 30 min (*C*) or 12 h (*D*), respectively. Images were analyzed with ImageJ software, and the surface area covered by the cells was normalized against the total number of the cells in each of the time points. The experiment was repeated with Tat-supplemented medium added at the 20th hour in *C* or at 0 h in *D*. The experiments were repeated at least two times; the results were analyzed by Student's *t* test; and statistical significance level ($p < 0.05$) is indicated by an *asterisk*, compared with the mock control group (one-way ANOVA test).

tors, such as BDNF and CREB proteins (28). Note that *BDNF* is a downstream target of CREB with multiple alternative transcription start sites, which are ultimately spliced to a single functional mature BDNF protein, and that exons I and IV of *BDNF* gene are transcriptional targets of CREB protein (29, 30).

These observations gave us the rationale to further study the impact of Tat on neuronal functions. Using qPCR, we examined expression levels of *BDNF* transcripts in Tat-treated SH-SY5Y cells. Quantitative RT-PCR analysis revealed that only exon IV, but not exon I, of the *BDNF* gene produced a transcript (Fig. 2*E*). As expected, BDNF-IV level decreases in Tat-treated cells at 24 h; however, it recovers at 48 h, which could be due to the half-life of Tat protein. These results agree with the axonal surface assay presented in Fig. 1*C*.

Next, we examined the level of CREB mRNA and protein in differentiated and treated SH-SY5Y cells. Similar to BDNF, the CREB level decreases in Tat-treated cells at 24 h and recovers at 48 h (Fig. 2*F*); however, CREB protein expression did not recover at 48 h as obtained by a Western blotting assay (Fig. 2*G*).

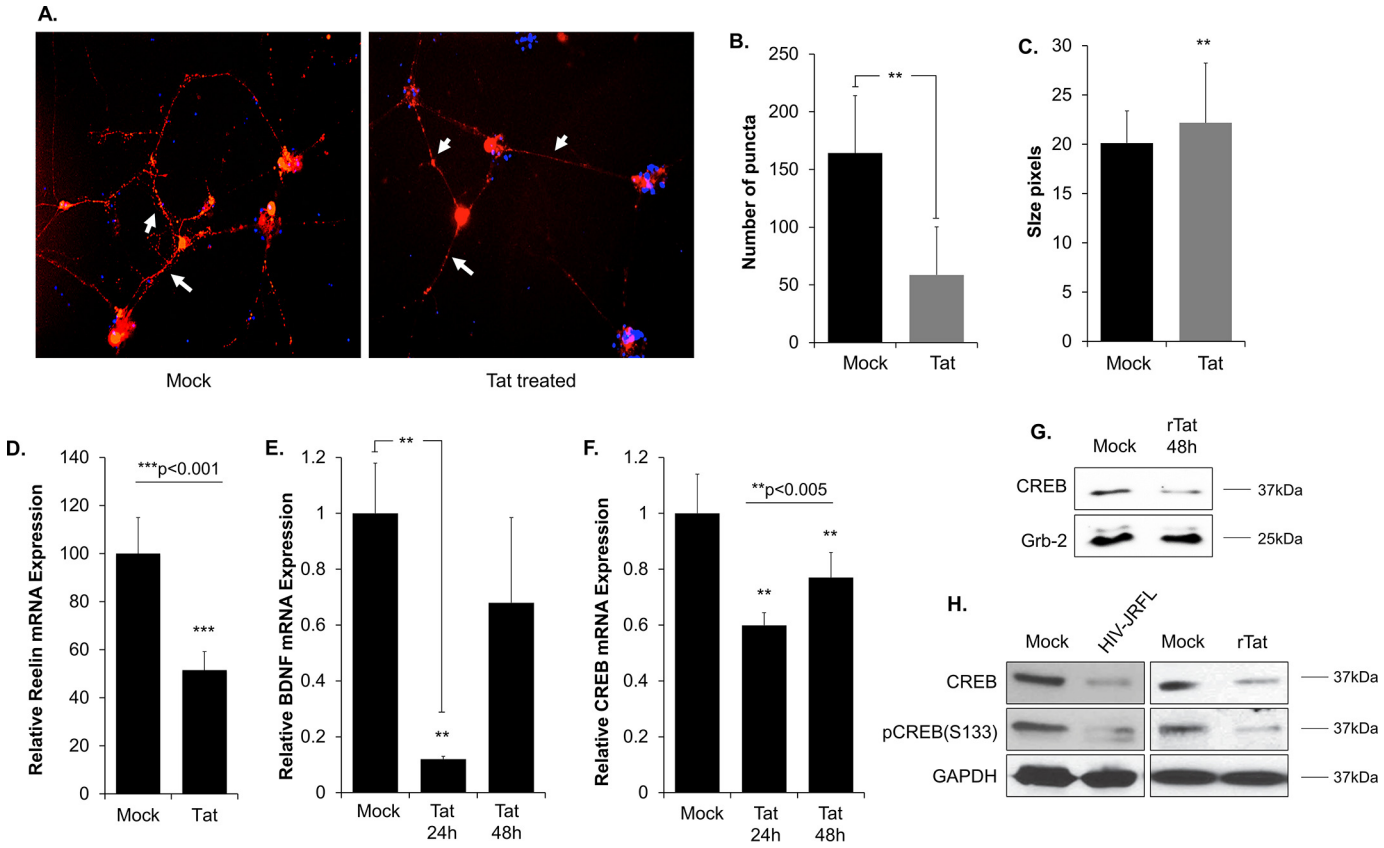

Figure 2. Tat alters the number and distribution of synaptophysin and expression levels of Reelin, CREB, and BDNF. *A*, representative images of synaptophysin vesicles (*red*) distribution in mouse primary neurons with or without Tat protein. Synaptophysin was expressed using Cell Light transduction at MOI 5. Tat protein or mock treatment was added 24 h after the transduction. Images of live cells were acquired at 24 h after Tat addition. DAPI (*blue*) was used to stain the nucleus. *B* and *C*, synaptophysin vesicle number and size were assessed using ImageJ for each condition. Images from at least 10 different fields were taken for statistical analysis. *D–F*, -fold changes of three selected genes (*Reelin*, *BDNF*, and *CREB*) involved in neurite retraction in Tat-treated SH-SY5Y cells compared with mock untreated obtained by qPCR. -Fold changes are displayed as histograms. Only 10 pg/ml rTat was used for treatment. *D*, Reelin; *E*, BDNF; *F*, CREB. Statistical analysis of parameters was performed using the one-way ANOVA test, followed by the unpaired Student's *t* test, with a *p* value less than 0.05 (as indicated by the *asterisk*) considered statistically significant. SH-SY5Y cells (5×10^5) (*G*) or primary human astrocytes (*H*) were treated with 10 pg/ml Tat protein for 48 h. Protein extracts were prepared from the cells or from primary astrocytes and used for Western blotting. Anti-CREB, -phospho-CREB(Ser-133), -Grb2, and -GAPDH antibodies were used as indicated.

Additionally, CREB protein depends on its ability to bind to the DNA (the promoter of the host gene) and not its increase/decrease in protein expression. CREB binding is ensured by the phosphorylation of its Ser-133 residue (31). Therefore, we determined whether the addition of HIV-1 and/or Tat protein affects CREB phosphorylation. Using a primary human culture of astrocytes, the cells were either infected with HIV-1 JR-FL strain for 10 days or treated with Tat protein for 48 h. The cells were collected, and the extracts were collected, where 50 μg of proteins were subjected to Western blot analysis using anti-CREB (total or phosphorylated Ser-133) and anti-GAPDH antibodies. As shown in Fig. 2*H*, infection of cells with HIV-1_{JRFL} or the addition of Tat protein led to a decrease in expression of total and/or phosphorylated CREB protein. Taken together, these results suggest that Tat protein can promote neurite retraction through reduction of CREB and BDNF expression levels.

Tat reduces CREB expression through E2F3

Because it is a downstream target of CREB protein, it is normal to observe a reduction in BDNF level if CREB is inhibited. However, one may question the mechanisms involved in CREB inhibition. In this regard, we previously demonstrated that up-regulation of miR-34a in Tat-treated SH-SY5Y leads to the inhibition of CREB mRNA and protein (5). It is well-known that miRNAs exhibit their function through partial complementary sequences located at the 3′-UTR of their target's mRNA. Those sequences are commonly referred to as seeds, and if miR-34a affects CREB expression, then it is logical for *CREB* 3′-UTR to contain miR-34a seeds. Unfortunately, neither bioinformatics analysis of the *CREB* 3′-UTR mRNA nor a literature search revealed or described such a site that could support our hypothesis.

Hence, we suspected the presence of an intermediate factor(s). To that end, we performed a *CREB* promoter analysis using ECR Browser for transcription factor–binding sites. The analysis displayed three highly conservative binding sites for Sp1, Egr, and E2F3 transcription factors (Fig. 3*A*). Sp1 binding to the *CREB* promoter was described previously (32), whereas EGR and E2F3 putative binding sites were only predicted. Further, TargetScan analysis of the 3′-UTR of the three transcription factors (Sp1, Egr, and E2F3) revealed that only *E2F3* contains seed for miR-34a (Fig. 3*B*, *yellow box*). Furthermore, *E2F3* has been shown to be a direct target of miR-34a, and the

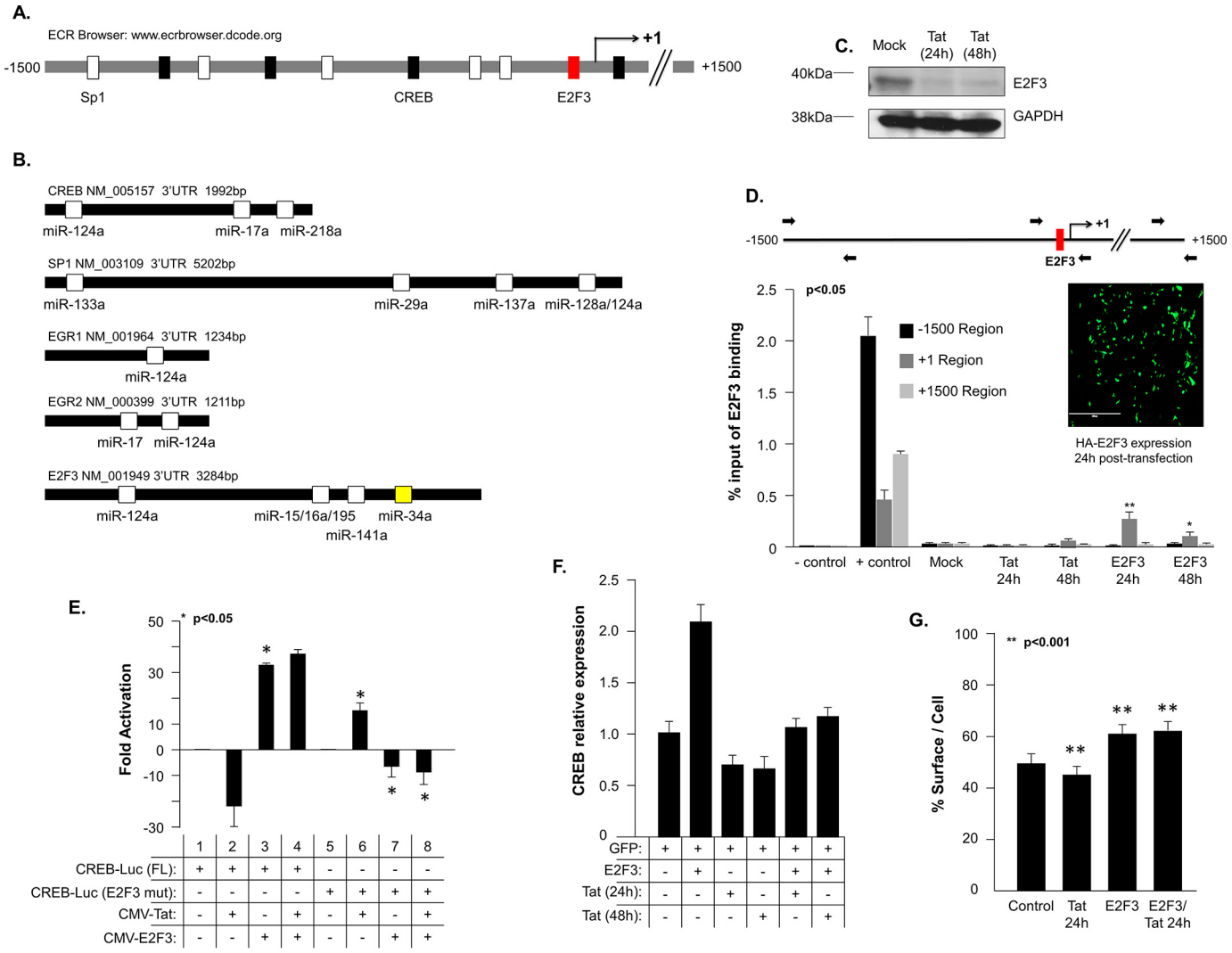

Figure 3. Identification of E2F3 as a new regulator of the *CREB* promoter. *A*, schematic representation of the CREB promoter. The potential binding sites are also shown. The presence of binding sites was verified using the literature and ECR Browser analysis for highly conserved putative binding sequences. *B*, *schematic display* of the 3′-UTR of known CREB, Sp1, or predicted Egr and E2F3 transcription factor mRNAs analyzed for potential miRNA-34a seeds (*yellow box*). *C*, Western blot analysis points to the ability of Tat to increase protein levels of E2F3 but not E2F1 in differentiated SH-SY5Y cells. Anti-E2F1, -E2F3, and -GAPDH antibodies were used as indicated. *D*, *schematic representation* of the *CREB* promoter with the positions of the various primers used for the ChIP assay. Binding of E2F3 to *CREB* DNA is also shown. Extracts prepared from SH-SY5Y cells transfected with plasmid expressing HA-E2F3 expression plasmid and then treated with Tat protein were subjected to a ChIP assay to evaluate the association of E2F3 with the *CREB* promoter DNA. *Inset*, transfection efficiency of the pcDNA-E2F3-HA plasmid at 24 h post-transfection. *E*, differentiated SH-SY5Y cells were transfected with 0.1 μg of *CREB*-luciferase (full-length or mutant) alone or in combination with 0.25 μg of E2F3 and/or Tat expression plasmids for 48 h. The cells were lysed and subjected to a luciferase assay. The experiment was repeated three times using different DNA preparations. The amount of DNA in each transfection mixture was normalized with pcDNA$_3$. *F*, -fold changes of *CREB* gene mRNA in SH-SY5Y cells transfected with E2F3 expression plasmid with or without Tat protein compared with mock untreated as obtained by qPCR. The experiment was repeated three times, and the results were statistically significant using Student's *t* test ($p < 0.05$) compared with the mock control group. *G*, following the same procedure as in Fig. 1*C*, surface area measurements of cells transfected with E2F3 expression plasmid with or without Tat protein compared with the mock untransfected and untreated.

functional relationship between *E2F3* and miR-34a has been established (33). Hence, we sought to examine whether decreased expression of CREB in Tat-treated cells is E2F3– and/or miR-34a– dependent.

To that end, we tested the impact of Tat protein on E2F3 expression in SH-SY5Y cells. Western blot analysis showed that the addition of Tat led to a decrease in E2F3 expression (Fig. 3*C*). GAPDH was used as a control for equal protein loading.

To further confirm the involvement of E2F3 in Tat-inducing CREB down-regulation, we performed a ChIP assay to examine the ability of E2F3 to bind to the predicted region of the *CREB* promoter. SH-SY5Y cells were transfected with E2F3-HA–tagged expression vector for 24 h, and then the cells were subjected to a ChIP assay. To discriminate against any nonspecific signal from the total E2F3-specific antibody, HA antibody was used. Several primers, covering three different regions from the CREB promoter, as displayed in Fig. 3*D* and described under "Experimental procedures," were used. As expected, untransfected or Tat-treated cells exhibit low or no binding, confirming the specificity of the antibody (Fig. 3*D*). E2F3 was able to interact with the +1 region of the *CREB* promoter and not with the other two regions that do not contain an E2F3-binding site. Efficiency of transfection

was controlled using GFP fluorescent plasmid (Fig. 3*D*, *inset*).

Next, we determined the ability of E2F3 to regulate the *CREB* promoter in the presence and absence of Tat. Using *CREB*-Luc full-length and mutant (where the E2F3 binding site was mutated; see "Experimental procedures") reporter plasmids, SH-SY5Y cells were transfected with 0.1 μg of *CREB*-Luc (FL or mutant) along with 0.25 μg of CMV-Tat and/or E2F3 expression plasmids. Luciferase assay results showed that the addition of Tat down-regulates the *CREB* promoter, whereas overexpression of E2F3 increased the *CREB* promoter expression, respectively (Fig. 3*E*, *lanes 2* and *3*). Interestingly, Tat failed to decrease the *CREB* promoter in the presence of E2F3 (Fig. 3*E*, *lane 4*). Similarly, Tat was unable to alter *CREB* gene regulation in the absence of the E2F3-binding site (*lane 6*). These results led to the conclusion that E2F3 is an important factor involved in *CREB* promoter regulation and that Tat protein exerts its negative effect through its functional (and maybe physical) interaction with the E2F3 transcription factor.

We validated these observations by performing an RT-qPCR. SH-SY5Y cells were transfected with 0.5 μg of HA-E2F3 expression plasmid and then treated with Tat protein for 24 and 48 h. The cells were collected, processed, and subjected to qPCR. As shown in Fig. 3*F*, overexpression of E2F3 modestly rescued CREB from being inhibited by Tat when compared with the mock untreated or with Tat-treated samples. GFP expression plasmid was used as a control to determine transfection efficacy.

At a functional level, using SH-SY5Y cells, we observed a larger area covered with elongated neurites in the presence of overexpressed E2F3 compared with the mock or Tat-treated cells (Fig. 3*G*). The addition of Tat and E2F3 did not affect neurite outgrowth. Taken together, these results pointed to a significant role of E2F3 in the CREB modification pathway.

E2F3 overexpression promotes CREB binding to the BDNF-IV promoter

Our results gave us the rationale to perform additional functional studies. Hence, we examined the impact of E2F3 overexpression on CREB and BDNF functional and physical interactions.

As described previously, the *BDNF* gene contains multiple alternative transcription start sites (34, 35) that are spliced together with a single protein-coding exon. Each of the alternative transcripts is under the regulation of a promoter sequence; however, only exons I and IV contain CREB protein response elements (36), as shown by ECR Browser promoter sequence analysis (Fig. 4*A*).

To determine whether E2F3 overexpression enables CREB binding to the CRE site within the *BDNF* promoter, SH-SY5Y cells were transfected with 0.5 μg of CMV-E2F3 expression plasmid. Transfected cells were collected at 24 and 48 h, processed, and subjected to a ChIP assay using anti-CREB antibody. As shown in Fig. 4*B*, an increase in CREB binding to the *BDNF-IV* promoter was observed in the presence of E2F3 compared with the mock untransfected. H3K9 was used a positive control.

To validate these results independently of Tat, we transfected SH-SY5Y cells with 0.1 μg of *BDNF-IV*-Luc (which contains three CRE-binding sites) alone or in the presence of an increasing amount of E2F3 or Sp1 expression plasmids as indicated. Sp1 transcription factor, used as a positive control, has been shown to enhance the *CREB* promoter. The cells were collected at 48 h after the transfection and subjected to a luciferase assay. As shown in Fig. 4*C*, E2F3 and/or Sp1 overexpression led to a significant activation (2–3-fold) of the *BDNF-IV* promoter when compared with the control.

Next, we attempted to link all of the partners to Tat. Therefore, we measured the mRNA expression levels of CREB and BDNF in the presence of Tat and E2F3. SH-SY5Y cells were transfected with E2F3 expression plasmid and then treated with HIV-1 Tat protein for 24 h. GFP plasmid was used as a positive control to determine transfection efficiency. mRNAs were collected and subjected to qPCR. As shown in Fig. 4*D*, overexpression of E2F3 was enough to prevent inhibition of *BDNF* and *CREB* genes when compared with the mock-transfected/untreated or Tat-treated samples.

Using anti-E2F3, -CREB, and -BDNF antibodies, similar results were obtained as revealed by Western blot analysis (Fig. 4*E*). The addition of Tat led to a decrease in the expression levels of E2F3, CREB, and BDNF proteins (compare *lane 3* with *lane 1*). However, the Tat negative effect was significantly reversed in the presence of overexpressed E2F3 (compare *lane 2* with *lane 3*). The percentage of increase/decrease of E2F3, CREB, and BDNF expressions are shown in Fig. 4*F*, as measured by densitometry. Anti-GAPDH antibody was used to control equal protein loading.

These results clearly explain the relation between Tat and neurite retraction. Additionally, these results led to the conclusion that Tat is using miR-34a to decrease expression levels of E2F3, leading to inhibition of CREB and BDNF, hence preventing neurite communications and eventually promoting neurocognitive disorders and premature brain aging.

Tat protein inhibits E2F3 through miR-34a

Because E2F3 is a downstream target of miR-34a, we sought to examine the exact role of miR-34a in this pathway. Further, it is well-described that miR-34a is a downstream target of p53 (37). Furthermore, we previously demonstrated the ability of HIV-1 Tat to up-regulate p53 protein (10). These results gave us the rationale to silence p53 and determine whether Tat exerts its negative effect on neurite retraction via 1) up-regulation of p53; 2) activation of miR-34a, a p53 target; 3) down-regulation of E2F3, a miR-34a downstream target; 4) inability of E2F3 to activate the *CREB* promoter; and 5) failure of CREB protein to activate the *BDNF-IV* promoter.

SH-SY5Y cells were transfected with small interfering RNA directed against the *p53* gene (siRNA-p53) and then treated with 10 ng/ml Tat protein for 24 h. The cells were collected and subjected to qPCR to examine the expression level of miR-34a and/or of *CREB* and *BDNF* genes. As shown in Fig. 5 (*A* and *B*), Tat failed to decrease expression levels of miR-34a (*A*) and of *CREB* and *BDNF* genes, respectively (*B*) in the absence of p53 when compared with the control.

The effects of Tat on p53 in the absence or the presence of siRNA-p53 were verified using a Western blotting assay, as shown in Fig. 5, *C* and *D*. SH-SY5Y cells were treated with Tat protein (*C*) in the presence and absence of nonspecific or small interfering RNA directed against *p53* (*D*). The expression level

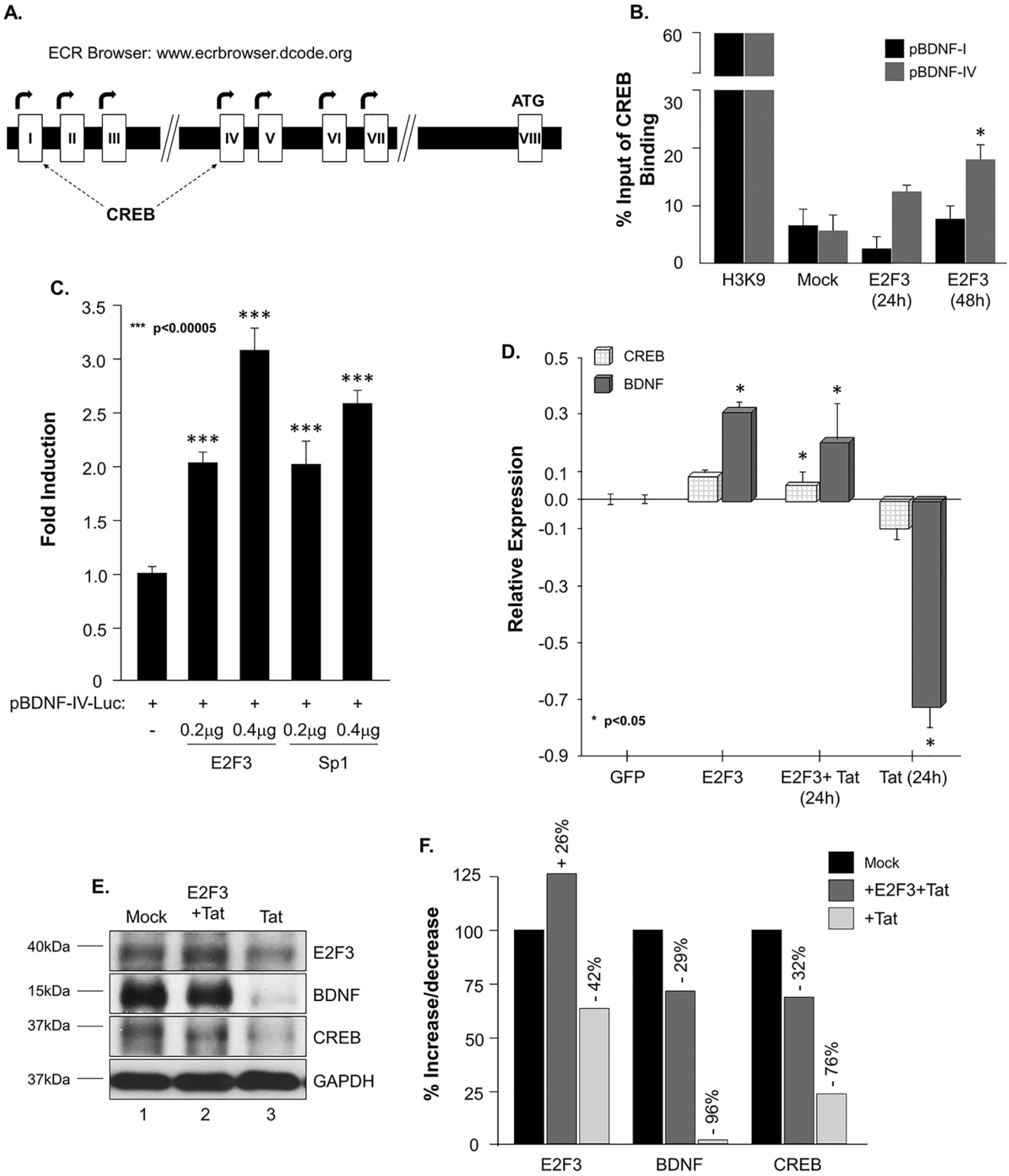

Figure 4. Effect of Tat and E2F3 on CREB-BDNF functional interplay. *A*, *schematic representation* of the human *BDNF* gene and its splicing variants. Only exon Is and IV contain a CREB-binding site. *B*, extracts prepared from SH-SY5Y cells were subjected to ChIP assay to evaluate the association of CREB with the *BDNF* promoters I and IV in the presence of overexpressed E2F3. *C*, SH-SY5Y cells were transfected with 0.1 μg of the *BDNF* IV-Luc full-length along with an increasing concentration of E2F3 or Sp1 expression plasmids, as indicated. The amount of DNA in each transfection mixture was normalized with pcDNA3. Luciferase activity was determined 48 h after transfection. Results are displayed as a histogram. *D*, -fold changes of CREB and BDNF mRNA in SH-SY5Y cells transfected with E2F3 expression plasmid and then treated with Tat protein compared with mock untransfected/untreated as obtained by qPCR. The experiment was repeated three times, and the results were statistically significant using Student's *t* test ($p < 0.05$) compared with the mock control group. *E*, Western blot analysis points to the ability of Tat to alter protein levels of E2F3, CREB, and BDNF. Anti-E2F3, -CREB, -BDNF, or -GAPDH antibodies were used as indicated. *F*, densitometric analyses were performed using EZQuant-Gel software (EZQuant Biology). The obtained data are expressed as the mean ± S.E.

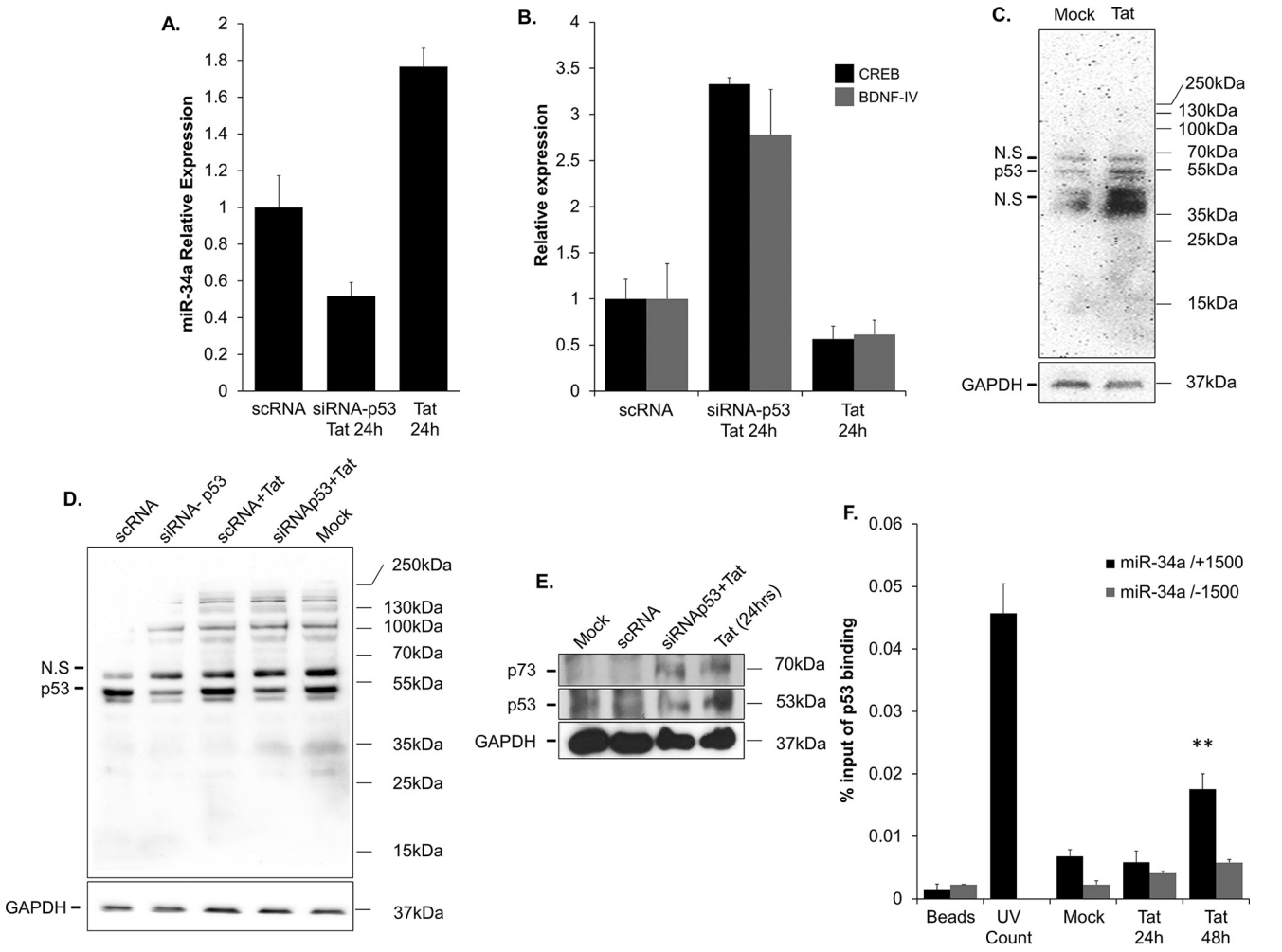

Figure 5. Tat suppresses E2F3 expression through induction of miR-34a. *A* and *B*, -fold changes of miR-34a (*A*) or CREB and BDNF (*B*) in SH-SY5Y cells transfected with siRNA-p53 with or without Tat protein compared with mock untreated cells obtained by qPCR. The experiment was repeated three times, and the results were statistically significant using Student's *t* test ($p < 0.05$) compared with the mock control group. *C–E*, Western blot analysis points to the ability of Tat to increase protein levels of p53 and p73. Tat failed to increase expression of p53 in the presence of siRNA-p53 but not of p73. Anti-p53, -p73, or -GAPDH antibodies were used as indicated. Scrambled RNA was used as a control. *F*, extracts prepared from SH-SY5Y cells were subjected to a ChIP assay to evaluate the association of p53 with the miR-34a promoter DNA (linc34a) in the absence or presence of Tat protein. As a positive control, cells were also subjected to UV light prior to the ChIP.

of p53 protein was detected by a Western blotting assay using anti-p53 or GAPDH antibodies. As shown, Tat induces expression of p53 (*C*); however, it failed to induce p53 in the presence of siRNA-p53 (*D*). The experiment was repeated three times using different cell passage numbers and different batches of Tat protein. Anti-GAPDH antibody was used to control equal protein loading.

We also examine the expression level of p73. The rationale for using p73 came from our previous studies, where we showed that Tat protein could induce expression of p53 protein through induction of the p73 protein. We also demonstrated that p53 is a downstream target of p73 and that inhibition of p53 will not affect the endogenous level of p73 (10, 38). As seen in Fig. 5*E* (*lanes 3* and *4*), Tat induces an endogenous level of p73 without being affected by siRNA-p53.

Further digging into the mechanisms involved led us to examine whether the addition of Tat enhances p53 binding to the miR-34a promoter (linc34a). Following the same procedure presented in Fig. 3*D*, a ChIP assay was performed using SH-SY5Y cells treated with Tat protein. As a positive control, one set of cells was exposed to UV light to induce endogenous p53. As shown in Fig. 5*F*, Tat enhances p53 binding to the miR-34a region +1500 and not to the region −1500. As expected, UV exposure increases the interaction of p53 to the +1500 region of the linc34a promoter. These results confirmed the specificity and the functional interplay between Tat, p53, and miR-34a.

E2F3 rescues Tat-induced synaptophysin distribution alteration

To further determine the functional role of E2F3, we examined whether it can reverse the loss of synaptic endings (see Fig. 1*C*). SH-SY5Y cells were transfected with E2F3 expression plasmid and then treated with Tat protein. As a control, $pcDNA_3$ empty vector was transfected. Interestingly, the number of synaptophysin vesicles (*red*) was higher in cells transfected with the empty vector, with E2F3 (Fig. 6*A*, *top panels*) and in cells transfected with E2F3 and treated with Tat protein (*bottom right panel*) when compared with cells treated with Tat (*bottom left panel*). Quantification and sizes of neurite (only) synpato-

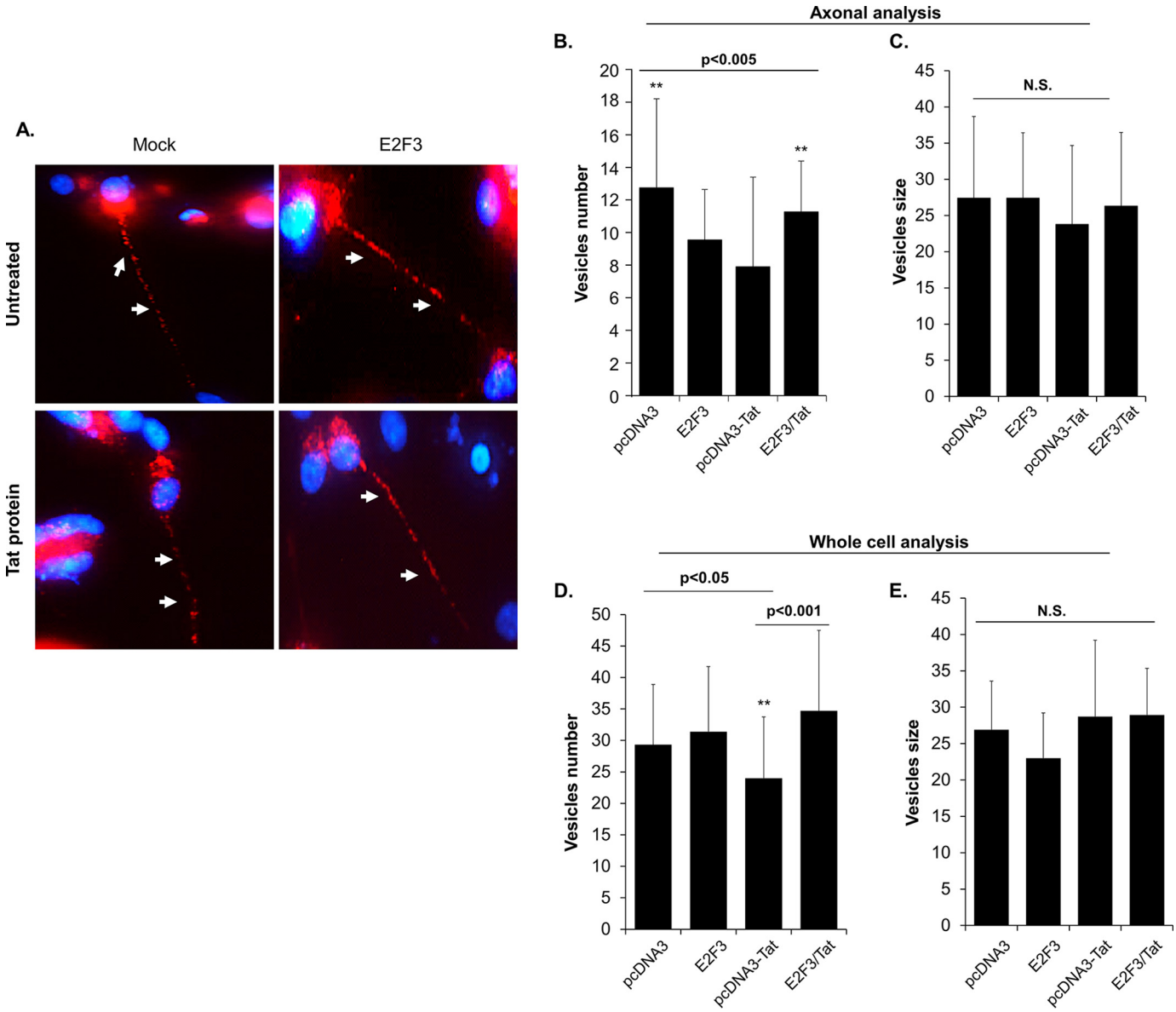

Figure 6. Distribution and quantification of synaptophysin in E2F3-transfected cells. *A*, representative images of synaptophysin vesicles (*red*) distribution in SH-SY5Y cells transfected with pcDNA3 empty vector or with E2F3 expression plasmid and then treated with Tat protein. Synaptophysin was expressed using Cell Light transduction at MOI 5. Tat protein or mock treatment was added 24 h after the transduction. Images of live cells were acquired at 24 h post-Tat addition. Transfection was performed prior to synaptophysin transduction. Nucleus were stained with DAPI (*blue*). *B–E*, synaptophysin vesicle number and size were assessed using ImageJ for each condition. Images from at least 10 different fields were taken for statistical analysis. The experiment was repeated three times, the results were analyzed by Student's *t* test, and statistical significance level ($p < 0.05$) is indicated by *asterisks*, compared with the mock control group (one-way ANOVA test). *N.S.*, not significant.

physin vesicles are presented in *B* and *C*, respectively. Nuclei were stained with DAPI (*blue*).

Further, quantification of the total number of vesicles (Fig. 6*D*), which includes cell body and neurite vesicles, revealed similar results as quantification of only the neurite synaptophysin vesicles (Fig. 6*E*). However, analysis of only neurite vesicles resulted in higher statistical significance. Taken together, these results point to the ability of HIV-1 Tat to promote neurite injury through a mechanism that implicates miR-34a and several proteins, mainly E3F3, the downstream target of miR-34a.

E2F3 and BDNF expression is reduced in HIVE brain

To validate our *in vitro* data, we sought to examine expression levels of E2F3 (*green*) and BDNF (*red*) proteins *in vivo*, using human brain tissues isolated from mock or from an HIV-1–infected patient with signs of encephalitis (HIVE). Using an immunohistochemistry assay, we observe that the expression level of E2F3 protein decreases in HIVE sections when compared with the mock uninfected sections (Fig. 7*A*). Nucleus were stained with DAPI (*blue*).

Distribution and subcellular localization of E2F3 and BDNF proteins were also examined by immunohistochemistry. As shown in Fig. 7*B*, in the uninfected section, E2F3 (green) was expressed ubiquitously with a perinuclear staining pattern, as indicated by the lack of color shift in the DAPI (*blue*) staining (*B*), whereas in the HIVE section, little or no E2F3-positive staining was observed. Similar results were obtained with BDNF (Fig. 7*B*, *BDNF panels*). Note that the

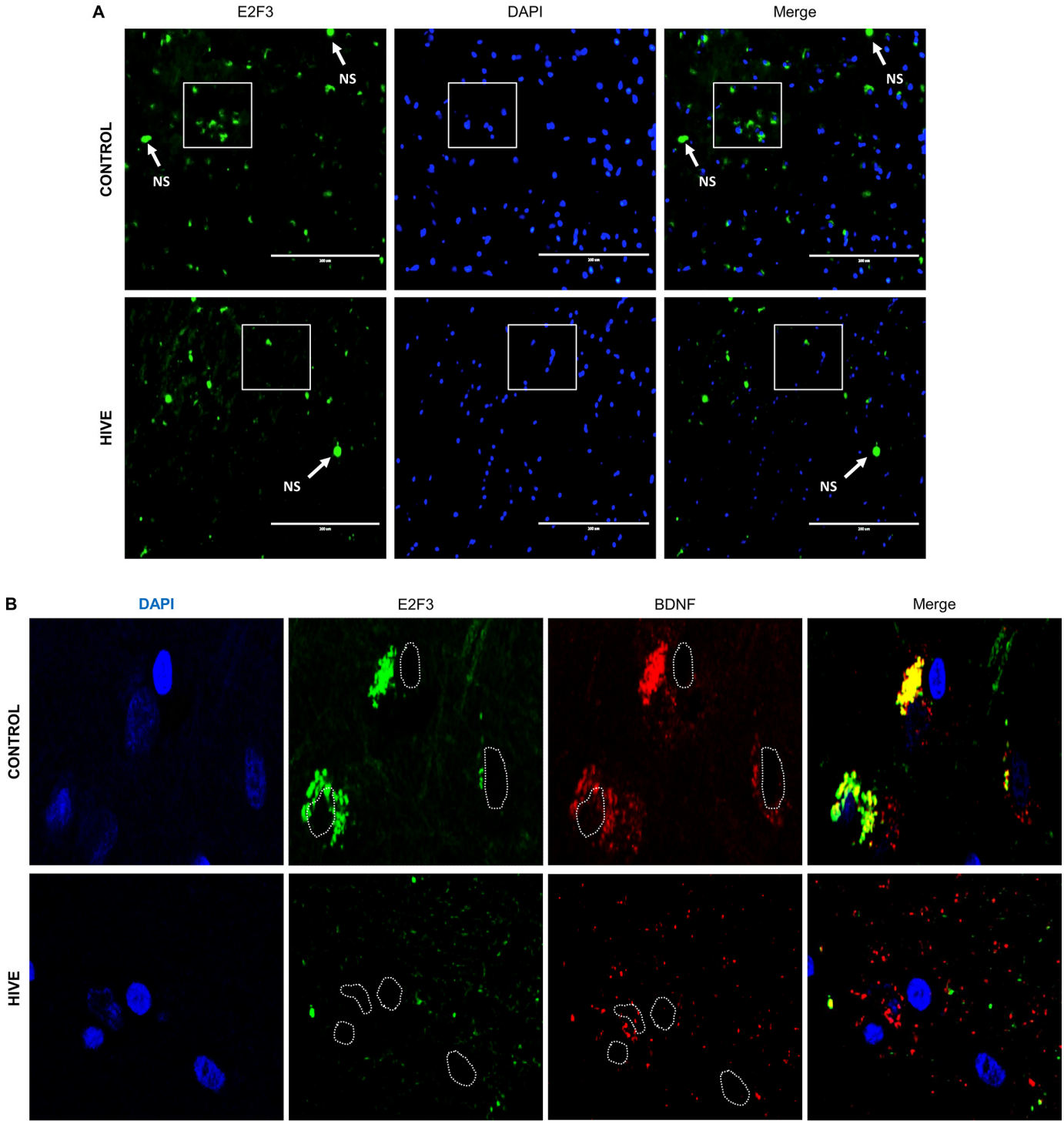

Figure 7. Immunohistochemistry assay depicting expression levels of E2F3 and BDNF protein. *A* and *B*, distribution and expression level of E2F3 (*green*; *A* and *B*) and BDNF (*red*; *B*) proteins in human brain tissue of an HIVE patient compared with the mock patient as obtained by immunohistochemistry assay. Nuclei were stained with DAPI (*blue*).

two proteins are localized in the cell compartment (*merge panel*).

Discussion

Failure of highly active antiretroviral therapy to lower the incidence rates of HAND provided the rationale to identify the molecular mechanisms involved. In this regard, HIV-1 Tat protein was shown to have the ability to induce neuronal cell dysfunction.

Here, we confirmed the negative role of Tat and its ability to promote neurite retraction. We also identified the cellular factors and the pathway involved. Interestingly, Tat triggered an action potential signal leading to the induction of the p53 protein and its downstream microRNA target, miR-34a (5). Acti-

vation of miR-34a turns out to have a domino effect on several downstream direct and indirect targets, such as E2F3, CREB, and BDNF, all of which are involved in neuronal communications (Figs. 1–6). We also confirmed the deregulation of these factors in human brain tissues isolated from an HIV-infected patient (Fig. 7) (see also Ref. 5). These results pointed to the key role that miR-34a and its target genes play in HIV-1–associated neurocognitive disorders.

The relation between miR34a and neuronal deregulation is not without precedent. It has been shown that an increase in miR-34a expression can alter hippocampal spinal morphology and function (39). Further, down-regulation of miR-34a was reported to have a positive impact on neuronal survival (40). Furthermore, activation of miR-34a was shown to be associated with the down-regulation of 136 genes involved in cell motility, energy production, and actin cytoskeleton organization, which indicates a critical role for miR-34a in neuronal precursor motility (41). miR-34a was also shown to increase cortical neuronal vulnerability to injury. In this regard, Truettner *et al.* (42) found that expression levels of miR-34a increase after traumatic brain injury and inhibit Bcl-2 and XIAP, both anti-apoptotic proteins. Additionally, miR-34a was found to be conserved between humans, mice, and rats during neuronal development and to play a role in mouse NS cell differentiation (43). Finally, increased miR-34a and its involvement in neurocognition are not limited to HIV-1. It has been shown that miR-34a is up-regulated in Alzheimer's disease and in schizophrenia and has a negative role in both diseases (44, 45).

Additionally, it has been reported that *E2F3* is a direct target of miR-34a (46). Interestingly, E2F3 has been described to have a negative effect on p53 expression (47). This observation confirmed the need of p53 to suppress E2F3 and to cause neuronal deregulation. These results further determine the major role that E2F3 might play in neuronal function in patients infected with HIV-1.

On the other hand, no reports describe a direct link between CREB and miR-34a. Further, despite the well-described relation between the E2F family and CREB, the relation between E2F3 and CREB has never been documented. In this regard, our data point to a new factor that could regulate the *CREB* promoter (Fig. 3*D*) and decipher the relation between CREB and miR-34a, a negative relation that led to neurite retraction and alteration of neuronal communication. Taken together, our results are considered a milestone that could partially explain the mechanisms leading to the development of neurocognitive disorders associated with HIV-1 infection.

However, one may ask what are the mechanisms used by Tat protein that trigger activation of p53. The answer to this question is summarized in Fig. 8. Based on our studies, HIV-1 Tat up-regulates p53 through a pathway that implicates down-regulation of miR-196a and activation of its downstream target, c-Abl, leading to the phosphorylation and activation of p73, which in turn activates p53. Note that the relationship between p73 and p53 was amply explored (48, 49); however, the role and impact of miR-196a on this association have never been explored. Further, it has been shown that induction of oxidative stress leads to activation of the c-Abl/p73 pathway (50). In this regard, several studies reported induction of the oxidative

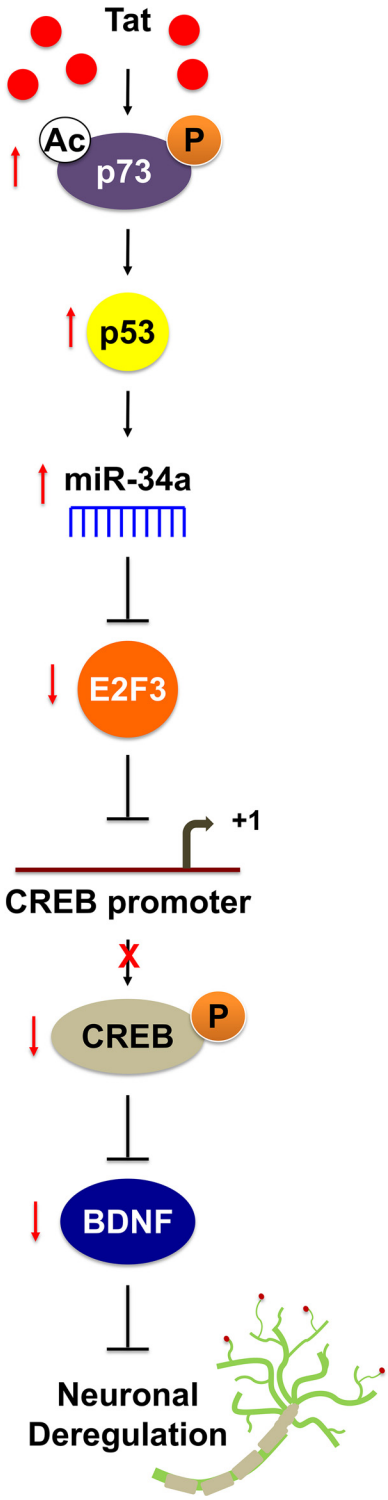

Figure 8. Pathway used by Tat leading to neurite retraction. Shown is a *schematic representation* of the pathway used by Tat leading to neurite retraction. All of the partners are shown.

stress pathway in Tat-treated human neurons (51), which explains our data regarding activation of the c-Abl and p73 proteins.

Interestingly, up-regulation of p53 led to modest cell death and a significant neurite retraction. The lack of significant cell death could be due to the ability of Tat to physically interact with the N-terminal domain of p73 and prevent it from causing

cell death (52). Global DNA methylation changes and methylation of *p73* and *p53* promoters could also provide an explanation for the lack of cell death. It has been shown that during aging phases, tumor suppressor factors are methylated and unable to perform their apoptotic functions (53). Our unpublished data[5] showed that Tat causes an increase in global DNA 5-hmC in SH-SY5Y cells, and this was also confirmed *in vivo* in Tat-transgenic mice, which corroborates with the literature. We are in the process of further exploring this avenue and examining the methylation status of the *p53* promoter.

It is noteworthy that other HIV-1 proteins, such as gp120 and Vpr, have been shown to cause neuronal damage (54). However, the mechanisms used by these two proteins are not fully understood and remain to be identified. Nevertheless, all three HIV-1 proteins use a pathway(s) that involved BDNF protein, which points to the importance of BDNF and the need to prevent its inhibition.

Overall, neurite retraction is an important cellular function that ensures neuronal communication and transfer of information, and its alteration leads to neuronal degeneration. Induction of neurite retraction has been shown to be somehow a general phenomenon associated with neuronal dysfunction. In this regard, several cellular factors have been shown to trigger neurite retraction, such as Rho, Wnt, accumulation of cytoplasmic calcium, and EP3. Therefore, it is necessary to investigate whether a common pathway exists between all of these proteins and whether the function of E2F3 is altered in these pathways.

Further, neurite retraction observed by HIV-1 Tat (Fig. 1) is not exclusive to HIV-1 and has been observed in other neurodegenerative diseases, such as Alzheimer's and Parkinson's disease. In this regard, it has been shown that lysophosphatidic acid has the capability to induce neurite retraction and Tau phosphorylation (55). Lysophosphatidic acid was also found to alter CREB protein expression (56). Neurite retraction associated with Alzheimer's disease was also noted in neuronal cells with increased PSD-95 protein or with a reduced amount of glyoxalase I activity (57, 58). In addition to HIV-1 and AD, neurite retraction was also described to be associated with Parkinson's disease through LRRK2 protein (59). Away from diseases, BDNF protein was found to inhibit hypoxia-induced neurite retraction by averting oxidative stress (60). Furthermore, it has been shown that Reelin prevents apical neurite retraction and can interact with APP to promote neurite outgrowth (61, 62). This last observation will be examined in the future studies. In addition, Reelin, BDNF, and CREB proteins have been shown to be involved in dendrite stability (63). Therefore, we concluded that by altering expression of Reelin, BDNF, and E2F3, Tat can also affect synaptic plasticity, which in turn could affect memory and promote HAND.

In summary, our data point to the pathway and the cellular players used by HIV-1 Tat protein to cause neurite retraction and neuronal damage. However, this is the first report, to our knowledge, to show involvement of E2F3 protein in neurite retraction and the development of HIV-1–associated neurocognitive disorders. Therefore, our data can serve as the basis for the development of a new molecular approach that could prevent progression and development of neurocognitive disorders associated with HIV-1.

[5] M. Santerre, A. Bagashev, L. Gorecki, K. Z. Lysek, Y. Wang, J. Shrestha, F. Del Carpio-Cano, R. Mukerjee, and B. E. Sawaya, unpublished data.

Experimental procedures

Reagents (antibodies, primers, and plasmids)

Fluo Am dyes were purchased from Invitrogen. Anti-E2F3, -HA, -BDNF, and -CREB or H3K9 antibodies were purchased from Santa Cruz Biotechnology, Inc. and Cell Signaling, respectively. pcDNA3-E2F3-HA was kindly received from Dr. Joseph R. Nevins (Duke University). pGL3-*BDNF-IV*-Luc plasmid was obtained as follows. *BDNF-IV* (1.3 kb) promoter sequence was synthetically generated by GenScript and received in a pUC57 backbone plasmid. The insert was released (NcoI/SacI) and inserted into the same sites into pGL3-Luciferase. Full-length (−1389/+172) pGL3-*CREB*-Luc plasmid was obtained by inserting human *CREB* promoter into KpnI/HindIII sites of pGL3-Luciferase. The insert was synthetically generated using the genomic DNA prepared from SH-SY5Y using the following primers: 5′- attaacggtaccgtccagaatcgaaccctctc-3′ (forward) and 5′-attaacaagctttcctcctcctgctcctcttac-3′ (reverse). *CREB*-Luc mutant (−1389/+172 mut (−174/−163)) was generated using the following primers: 5′- gctttaccgatgcgaaaggaattctggagtttagaccactcc-3′ (forward) and 5′-ggagtggtctaaactccagaattcctttcgcatcggtaaagc-3′ (reverse).

Tat protein

Recombinant full-length Tat protein was obtained through the National Institutes of Health AIDS Reagent Program, Division of AIDS: HIV-1 IIIB Tat recombinant protein without a tag. The protein was lyophilized in PBS and resuspended in Teknova molecular biology grade water. Control wells received an equal volume of the vehicle alone (10× PBS (Corning, Cellgro) diluted to 1× with Teknova molecular biology grade water, certified negative for DNase and RNase and nonspecific endonuclease, exonuclease, and protease activity).

Cell culture and treatments

SH-SY5Y neuroblastoma cells were maintained in F-12/DMEM (50/50) supplemented with sodium pyruvate, nonessential amino acids, and 10% FBS final concentration. Cells were seeded in 50% confluence and differentiated with 10 μM retinoic acid for at least 48 h prior to Tat treatment (10 ng/ml final concentration). Only SH-SY5Y cells in passages 25–35 were used.

Primary cultures

Primary neuronal cultures or primary astrocytes were prepared as described previously (64) with minor modifications. Briefly, embryos were removed from mice at embryonic day 18. The cortex was separated and rinsed in Hanks' balanced salt solution before it was digested in 0.125% trypsin. The digested cortex was triturated and dissociated into a single-cell suspension in culture medium (DMEM containing 10% FBS). Cell suspension was centrifuged at 200 × *g* for 10 min, and the pellet was gently resuspended in culture medium. The cell suspension was passed through mesh 400 to remove the nondispersed tis-

sue, and the cells were seeded at a density of 1.5×10^5 cells/ml into 4-chamber slides coated with poly-D-lysine. Cultures were incubated in an incubator at 37 °C in an atmosphere of 5% CO_2 in air. The medium was changed into Neurobasal supplemented with 2% B27 and 0.5 mM glutamine the next day. Half of the medium was changed every 3 days.

Transfection and luciferase assay

For the transfection assay, 5×10^5 cells (SH-SY5Y) were resuspended in Lonza P3 medium (catalog no. V4XP3012) with 3 μg of endotoxin-free DS-Red expression plasmid and electroporated using a 4D-Nucleofector™ X unit. Cells were seeded (8×10^5) in 35-mm dishes or plates coated with poly-D-lysine (Sigma-Aldrich). Cultures were incubated at 37 °C incubator containing 5% CO_2. Twenty-four hours later, the cells were washed with Hanks' balanced salt solution, and the medium was replaced with neuron-specific medium (Neurobasal + 2% B27, 1× GlutaMAX, 1× nonessential amino acids, 50 IU/ml penicillin and streptomycin; Invitrogen). The medium was changed every 3 days. Recombinant Tat was added to the culture on days 5 and 7, and neurons were collected or recorded on day 9.

SH-SY5Y cells (2×10^5) were transfected with 0.1 μg of *CREB*-luciferase reporter plasmids (FL or mutant) using Lipofectamine® 2000 (Thermo Fisher Scientific) along with 0.25 μl of CMV-E2F3 and/or CMV-Tat expression plasmids for 48 h. The cells were washed, collected, and processed for the luciferase assay using the Berthold detection system. Three independent experiments were conducted.

ChIP

SH-SY5Y cells (10^7) were transfected and/or treated with HIV-1 Tat protein and subsequently were fixed with 1% formaldehyde (final concentration) for 15 min, followed by 125 mM glycine (final concentration) for 10 min at room temperature. Cells were then washed twice, incubated for 30 min on ice, and sonicated to shear the DNA. After sonication, the lysates were centrifuged, and the supernatants were diluted. The chromatin was immunoprecipitated with anti-CREB, anti-E2F3, anti-H3K9, or anti-p53 antibodies. Antibodies were eluted from the immune complexes, and cross-linking was reversed by heating at 65 °C overnight. The following specific primers were used: +1 *CREB* site, 5′-agcctgccgtgtggtcat-3′ (sense) and 5′-tgaagctgggactcccccaacc-3′ (antisense); +1600 *CREB* site, 5′-atagaaggcatgacacgggaacc-3′ (sense) and 5′-ccgagggaaaaccaaaacagcactcat-3′ (antisense); −1600 *CREB* site, 5′-ccagggatacacagagaaacc-3′ (sense) and 5′-gtcagagtgaggccatagatg-3′ (antisense); *BDNF4*, 5′-tggggttgggggagtcccag-3′ (sense) and 5′-acccgtgctggcctttcagc-3′ (antisense); *BDNF1*, 5′-aggcatgacacgggaaccagact-3′ (sense) and 5′-agaggcctaggtcgggacaca-3′ (antisense); miR-34a (−1500), 5′-aacatgggctcatcacagacacct-3′ (sense) and 5′-aggtgcgtaatcacatttgggcac-3′ (antisense); miR-34a (+1500), 5′-taagtgcaaaggccctgtgtttgg-3′ (sense) and 5′-agctgcagtactgatgtgtgctct-3′ (antisense).

RNA isolation and quantitative real-time PCR

Total RNA was isolated by using TRIzol reagent, following the manufacturer's protocol. For mRNA quantification, cDNA was synthesized using SuperScript® VILO™ cDNA synthesis kit. Quantitative real-time PCR was performed in triplicate using Faststart universal SYBR Green mix (Roche Applied Science) on an Eco system (Illumina). The mRNA level was normalized to glyceraldehyde-3-phosphate dehydrogenase (*GAPDH*) as a housekeeping gene. The following human primers were used: miR-34a, Primer mix (Exiqon); *GAPDH*, 5′-tcgacagtcagccgcatcttcttt-3′ (sense) and 5′-accaaatccgttgactccgacctt-3′ (antisense); *CREB*, 5′-aaagcagtgacggaggagcttgta-3′ (sense) and 5′-ggctgggcttgaactgtcatttgt-3′ (antisense); *BDNF* exon 1, 5′-tggttcttctgctctgctgtgcta-3′ (sense) and 5′-tccggaaatctcgggaaataggca-3′ (antisense); *BDNF* exon 2, 5′-tagcggtgtaggctggaatagact-3′ (sense); *BDNF* exons 1 and 2, 5′-ggcagccttcatgcaaccaaagta-3′ (antisense); *BDNF* exon 3, 5′-cttagagggttcccgctttctcaa-3′ (sense); *BDNF* exon 4, 5′-gagcagctgccttgatggttacct-3′ (sense); *BDNF* exons 3 and 4, 5′-aagccaccttgtcctcggatgttt-3′ (antisense).

Visualization and measurement of synaptophysin

Primary neuronal cells were cultured for 5 days before they were transduced with CellLight Synaptophysin-RFP BacMam at an MOI of 5. Cells were then cultured for an additional 24 h before Tat (10 ng/ml) protein was added. Images were acquired on live cells 24 h after Tat treatment. Images were processed; synaptophysin vesicle number and size were quantified with ImageJ software using the Compute Curvatures and Analyze Particles plugins. Images from at least 10 different fields of two independent experiments were used for statistical analysis.

Live cell imaging

Images of differentiated and Tat-treated SH-SY5Y cells or mock- and Tat-treated primary mouse neurons grown in 100-cm^2 dishes were taken every 30 min for 96 h (SH-SY5Y) or every 12 h for 48 h (primary mouse neurons) using an EVOS AMD microscope (×40 objective) installed inside the incubator. Images were analyzed using ImageJ software. Each image was then analyzed with the Compute Curvature plugin with Gaussian convolution σ parameter set at 1, followed by a conversion to a binary image and finally surface area of the cells analyzed with the Measure function. Surface area was expressed as the percentage of covered surface per cell.

Fluo3 calcium indicator assay

Fluo3 in 5 mM working solution containing 0.02% Pluronic in DMSO was added to the differentiated and Tat-treated SH-SY5Y cell medium for a final concentration of 5 μM for 30 min at 37 °C. Cells were then washed three times with 1 ml of medium. A confocal microscope equipped with a live cell imaging setting was then used.

Immunohistochemistry

Frontal lobe brain tissues from HIV-positive patients with varying degrees of dementia, along with nondemented and HIV-negative controls, were obtained from the National NeuroAIDS Tissue Consortium. The formalin-fixed and paraffin-embedded tissues were sectioned at 5-μm thickness and placed on electromagnetically charged glass slides. Sections were deparaffinized in xylene and rehydrated through descending

grades of alcohol up to water. Nonenzymatic antigen retrieval was performed in citrate buffer for 30 min at 95 °C in a vacuum oven. Sections were then rinsed with PBS and permeabilized in 0.2% Triton in PBS for 45 min at room temperature. Sections were rinsed again with PBS, and a blocking step was performed with normal BSA serum at room temperature in a humidified chamber for 2 h. Primary antibodies were incubated overnight at 4 °C and later for 1 h at room temperature with fluorescently labeled secondary antibodies. The tissues were subsequently washed in PBS until finally mounted with DAPI-containing medium (Vectashield).

Immunofluorescence

Cells were fixed for 3 min in 2% paraformaldehyde, rinsed with PBS, and blocked with 1% BSA for 1 h. A specific primary antibody (1:100 dilution) was incubated for 2 h at room temperature (or overnight at 4 °C), after which cells were incubated with a fluorescein-tagged secondary antibody for 1 h at room temperature. Cells were then washed and mounted with DAPI-containing medium. A LEICA EL6000 DMI3000 confocal microscope system was used with a UV laser (405-nm wavelength), an argon laser (488-nm wavelength), and an HeNe laser (543- and 633-nm wavelength). *Z*-Sections at a depth of 0.25–0.45 mm were generated. In some cases, contrast and/or intensity was adjusted to improve comparison of different stains. When applied, these changes affected the entire panel.

Western blotting

Samples were lysed in radioimmune precipitation assay buffer. Twenty micrograms of total extracts were subjected to Western blot analysis using specific antibodies as indicated. Densitometry analysis of the gels was carried out by using ImageJ software.

HIV-1 infection

Primary human astrocytes was maintained in DMEM + 10% FBS, 100 units/ml penicillin, 50 μg/ml streptomycin-G. Cells in log phase were infected with JR-FL strains of HIV-1 as follows. Fifty nanograms of p24-containing virus stock were added per 1×10^6 cells. Cells were incubated with virus stock in a small volume of serum-free medium for 2 h at 37 °C. The cells were then washed twice with PBS, and fresh medium containing 2% of FBS was added (500,000 cells/ml). All infection experiments were performed three times.

Statistics and bioinformatics

Statistical analyses were used in all the experiments using Student's *t* tests or unbalanced analysis of variance. Further, one-way ANOVA was also used to confirm the results. Furthermore, each experiment was repeated three times, and the results were considered statistically significant if p was <0.05. All results are expressed as mean ± S.D. PubMed and Ensembl were used to identify promoter and gene coding regions. ECR Genome Browser (http://ecrbrowser.dcode.org/)[6] (65) and Target Scan Human (http://www.targetscan.org/vert_61/docs/help.html)[6] were used for transcription factor–binding site and miRNA prediction identification.

[6] Please note that the JBC is not responsible for the long-term archiving and maintenance of this site or any other third party hosted site.

Author contributions—A. B. and M. S. designed and performed experiments and wrote the manuscript; L. G., K. Z. L., Y. W., F. D. C.-C., J. S., and R. M. performed experiments; B. E. S. designed experiments, analyzed the data, and wrote the manuscript.

Acknowledgments—The following reagent was obtained through the AIDS Research and Reference Reagent Program, Division of AIDS, NIAID, National Institutes of Health: Tat protein.

References

1. Gorantla, S., Poluektova, L., and Gendelman, H. E. (2012) Rodent models for HIV-associated neurocognitive disorders. *Trends Neurosci.* **35,** 197–208 CrossRef Medline
2. del Palacio, M., Alvarez, S., and Muñoz-Fernández, M. Á. (2012) HIV-1 infection and neurocognitive impairment in the current era. *Rev. Med. Virol.* **22,** 33–45 CrossRef Medline
3. Valcour, V. G. (2013) HIV, aging, and cognition: emerging issues. *Top. Antivir. Med.* **21,** 119–123 Medline
4. Mayne, M., Holden, C. P., Nath, A., and Geiger, J. D. (2000) Release of calcium from inositol 1,4,5-trisphosphate receptor-regulated stores by HIV-1 Tat regulates TNF-α production in human macrophages. *J. Immunol.* **164,** 6538–6542 CrossRef Medline
5. Chang, J. R., Mukerjee, R., Bagashev, A., Del Valle, L., Chabrashvili, T., Hawkins, B. J., He, J. J., and Sawaya, B. E. (2011) HIV-1 Tat protein promotes neuronal dysfunction through disruption of microRNAs. *J. Biol. Chem.* **286,** 41125–41134 CrossRef Medline
6. Li, W., Li, G., Steiner, J., and Nath, A. (2009) Role of Tat protein in HIV neuropathogenesis. *Neurotox. Res.* **16,** 205–220 CrossRef Medline
7. Ensoli, B., Buonaguro, L., Barillari, G., Fiorelli, V., Gendelman, R., Morgan, R. A., Wingfield, P., and Gallo, R. C. (1993) Release, uptake, and effects of extracellular human immunodeficiency virus type 1 Tat protein on cell growth and viral transactivation. *J. Virol.* **67,** 277–287 Medline
8. Kolson, D. L., Collman, R., Hrin, R., Balliet, J. W., Laughlin, M., McGann, K. A., Debouck, C., and Gonzalez-Scarano, F. (1994) Human immunodeficiency virus type 1 Tat activity in human neuronal cells: uptake and trans-activation. *J. Gen. Virol.* **75,** 1927–1934 CrossRef Medline
9. Self, R. L., Mulholland, P. J., Nath, A., Harris, B. R., and Prendergast, M. A. (2004) The human immunodeficiency virus type-1 transcription factor Tat produces elevations in intracellular is Ca^{2+} that require function of an *N*-methyl-D-aspartate receptor polyamine-sensitive site. *Brain Res.* **995,** 39–45 CrossRef Medline
10. Mukerjee, R., Deshmane, S. L., Fan, S., Del Valle, L., White, M. K., Khalili, K., Amini, S., and Sawaya, B. E. (2008) Involvement of the p53 and p73 transcription factors in neuroAIDS. *Cell Cycle* **7,** 2682–2690 CrossRef Medline
11. Fitting, S., Booze, R. M., and Mactutus, C. F. (2008) Neonatal intrahippocampal injection of the HIV-1 proteins gp120 and Tat: differential effects on behavior and the relationship to stereological hippocampal measures. *Brain Res.* **1232,** 139–154 CrossRef Medline
12. Kim, B. O., Liu, Y., Ruan, Y., Xu, Z. C., Schantz, L., and He, J. J. (2003) Neuropathologies in transgenic mice expressing human immunodeficiency virus type 1 tat protein under the regulation of the astrocyte-specific glial fibrillary acidic protein promoter and doxycycline. *Am. J. Pathol.* **162,** 1693–1707 CrossRef Medline
13. Hayman, M., Arbuthnott, G., Harkiss, G., Brace, H., Filippi, P., Philippon, V., Thomson, D., Vigne, R., and Wright, A. (1993) Neurotoxicity of peptide analogues of the transactivating protein tat from Maedi-Visna virus and human immunodeficiency virus. *Neuroscience* **53,** 1–6 CrossRef Medline
14. Everall, I., Barnes, H., Spargo, E., and Lantos, P. (1995) Assessment of neuronal density in the putamen in human immunodeficiency virus infection: application of stereology and spatial analysis of quadrats. *J. Neurovirol.* **1,** 126–129 CrossRef Medline

15. Cheng, J., Nath, A., Knudsen, B., Hochman, S., Geiger, J. D., Ma, M., and Magnuson, D. S. K. (1998) Neuronal excitatory properties of human immunodeficiency virus type 1 Tat protein. *Neuroscience* **82,** 97–106 Medline
16. Kida, S. (2012) A functional role for CREB as a positive regulator of memory formation and LTP. *Exp. Neurobiol.* **21,** 136–140 CrossRef Medline
17. Zhao, Y.-N., Li, W.-F., Li, F., Zhang, Z., Dai, Y.-D., Xu, A.-L., Qi, C., Gao, J.-M., and Gao, J. (2013) Resveratrol improves learning and memory in normally aged mice through microRNA-CREB pathway. *Biochem. Biophys. Res. Commun.* **435,** 597–602 CrossRef Medline
18. Edelmann, E., Lessmann, V., and Brigadski, T. (2014) Pre- and postsynaptic twists in BDNF secretion and action in synaptic plasticity. *Neuropharmacology* **76,** 610–627 Medline
19. Marambaud, P., Dreses-Werringloer, U., and Vingtdeux, V. (2009) Calcium signaling in neurodegeneration. *Mol. Neurodegener.* **4,** 20 CrossRef Medline
20. Lipton, S. A. (1994) HIV-related neuronal injury. Potential therapeutic intervention with calcium channel antagonists and NMDA antagonists. *Mol. Neurobiol.* **8,** 181–196 CrossRef Medline
21. Lipton, S. A. (1994) Neuronal injury associated with HIV-1 and potential treatment with calcium-channel and NMDA antagonists. *Dev. Neurosci.* **16,** 145–151 CrossRef Medline
22. Li, H., Zhong, X., Chau, K. F., Williams, E. C., and Chang, Q. (2011) Loss of activity-induced phosphorylation of MeCP2 enhances synaptogenesis, LTP and spatial memory. *Nat. Neurosci.* **14,** 1001–1008 CrossRef Medline
23. Dailey, M. E., Buchanan, J., Bergles, D. E., and Smith, S. J. (1994) Mossy fiber growth and synaptogenesis in rat slices *in vitro*. *J. Neurosci.* **14,** 1060–1078 Medline
24. Dijkhuizen, P. A., and Ghosh, A. (2005) BDNF regulates primary dendrite formation in cortical neurons via the PI3-kinase and MAP kinase signaling pathways. *J. Neurobiol.* **62,** 278–288 CrossRef Medline
25. Weeber, E. J., Beffert, U., Jones, C., Christian, J. M., Forster, E., Sweatt, J. D., and Herz, J. (2002) Reelin and ApoE receptors cooperate to enhance hippocampal synaptic plasticity and learning. *J. Biol. Chem.* **277,** 39944–39952 CrossRef Medline
26. Impagnatiello, F., Guidotti, A. R., Pesold, C., Dwivedi, Y., Caruncho, H., Pisu, M. G., Uzunov, D. P., Smalheiser, N. R., Davis, J. M., Pandey, G. N., Pappas, G. D., Tueting, P., Sharma, R. P., and Costa, E. (1998) A decrease of reelin expression as a putative vulnerability factor in schizophrenia. *Proc. Natl. Acad. Sci. U.S.A.* **95,** 15718–15723 CrossRef Medline
27. Huang, E. J., and Reichardt, L. F. (2001) Neurotrophins: roles in neuronal development and function. *Annu. Rev. Neurosci.* **24,** 677–736 CrossRef Medline
28. Sakamoto, K., Karelina, K., and Obrietan, K. (2011) CREB: a multifaceted regulator of neuronal plasticity and protection. *J. Neurochem.* **116,** 1–9 CrossRef Medline
29. Kwon, M., Fernández, J. R., Zegarek, G. F., Lo, S. B., and Firestein, B. L. (2011) BDNF-promoted increases in proximal dendrites occur via CREB-dependent transcriptional regulation of cypin. *J. Neurosci.* **31,** 9735–9745 CrossRef Medline
30. Lesiak, A., Pelz, C., Ando, H., Zhu, M., Davare, M., Lambert, T. J., Hansen, K. F., Obrietan, K., Appleyard, S. M., Impey, S., and Wayman, G. A. (2013) A genome-wide screen of CREB occupancy identifies the RhoA inhibitors Par6C and Rnd3 as regulators of BDNF-induced synaptogenesis. *PLoS One* **8,** e64658 CrossRef Medline
31. Shaywitz, A. J., Dove, S. L., Kornhauser, J. M., Hochschild, A., and Greenberg, M. E. (2000) Magnitude of the CREB-dependent transcriptional response is determined by the strength of the interaction between the kinase-inducible domain of CREB and the KIX domain of CREB-binding protein. *Mol. Cell. Biol.* **20,** 9409–9422 CrossRef Medline
32. Walker, W. H., Fucci, L., and Habener, J. F. (1995) Expression of the gene encoding transcription factor cyclin adenosine 3′,5′-monophosphate (cAMP) response element binding protein (CREB): regulation by follicle-stimulating hormone-induced cAMP signaling in primary rat Sertoli cells. *Endocrinology* **136,** 3534–3545 CrossRef Medline
33. Welch, C., Chen, Y., and Stallings, R. L. (2007) MicroRNA-34a functions as a potential tumor suppressor by inducing apoptosis in neuroblastoma cells. *Oncogene* **26,** 5017–5022 CrossRef Medline
34. Timmusk, T., and Metsis, M. (1994) Regulation of BDNF promoters in rat hippocampus. *Neurochem. Int.* **25,** 11–15 CrossRef Medline
35. Timmusk, T., Palm, K., Metsis, M., Reintam, T., Paalme, V., Saarma, M., and Persson, H. (1993) Multiple promoters direct tissue specific expression of the rat BDNF gene. *Neuron* **10,** 475–489 CrossRef Medline
36. Tabuchi, A., Sakaya, H., Kisukeda, T., Fushiki, H., and Tsuda, M. (2002) Involvement of an upstream stimulatory factor as well as cAMP-responsive element-binding protein in the activation of brain-derived neurotrophic factor gene promoter I. *J. Biol. Chem.* **277,** 35920–35931 CrossRef Medline
37. Raver-Shapira, N., Marciano, E., Meiri, E., Spector, Y., Rosenfeld, N., Moskovits, N., Bentwich, Z., and Oren, M. (2007) Transcriptional activation of miR-34a contributes to p53-mediated apoptosis. *Mol. Cell* **26,** 731–743 CrossRef Medline
38. Bagashev, A., Mukerjee, R., Santerre, M., Del Carpio-Cano, F. E., Shrestha, J., Wang, Y., He, J. J., and Sawaya, B. E. (2014) Involvement of miR-196a in HIV-associated neurocognitive disorders. *Apoptosis* **19,** 1202–1214 CrossRef Medline
39. Agostini, M., Tucci, P., Steinert, J. R., Shalom-Feuerstein, R., Rouleau, M., Aberdam, D., Forsythe, I. D., Young, K. W., Ventura, A., Concepcion, C. P., Han, Y.-C., Candi, E., Knight, R. A., Mak, T. W., and Melino, G. (2011) microRNA-34a regulates neurite outgrowth, spinal morphology, and function. *Proc. Natl. Acad. Sci. U.S.A.* **108,** 21099–21104 CrossRef Medline
40. Khanna, A., Muthusamy, S., Liang, R., Sarojini, H., and Wang, E. (2011) Gain of survival signaling by down-regulation of three key miRNAs in brain of calorie-restricted mice. *Aging* **3,** 223–236 CrossRef Medline
41. Chang, S. J., Weng, S. L., Hsieh, J. Y., Wang, T. Y., Chang, M. D., and Wang, H. W. (2011) MicroRNA-34a modulates genes involved in cellular motility and oxidative phosphorylation in neural precursors derived from human umbilical cord mesenchymal stem cells. *BMC Med. Genomics* **4,** 65 CrossRef Medline
42. Truettner, J. S., Motti, D., and Dietrich, W. D. (2013) MicroRNA overexpression increases cortical neuronal vulnerability to injury. *Brain Res.* **1533,** 122–130 CrossRef Medline
43. Aranha, M. M., Santos, D. M., Xavier, J. M., Low, W. C., Steer, C. J., Solá, S., and Rodrigues, C. M. P. (2010) Apoptosis-associated microRNAs are modulated in mouse, rat and human neural differentiation. *BMC Genomics* **11,** 514 CrossRef Medline
44. Wang, X., Liu, P., Zhu, H., Xu, Y., Ma, C., Dai, X., Huang, L., Liu, Y., Zhang, L., and Qin, C. (2009) miR-34a, a microRNA up-regulated in a double transgenic mouse model of Alzheimer's disease, inhibits bcl2 translation. *Brain Res. Bull.* **80,** 268–273 CrossRef Medline
45. Kim, A. H., Reimers, M., Maher, B., Williamson, V., McMichael, O., McClay, J. L., van den Oord, E. J., Riley, B. P., Kendler, K. S., and Vladimirov, V. I. (2010) MicroRNA expression profiling in the prefrontal cortex of individuals affected with schizophrenia and bipolar disorders. *Schizophr. Res.* **124,** 183–191 CrossRef Medline
46. Reimer, D., Hubalek, M., Kiefel, H., Riedle, S., Skvortsov, S., Erdel, M., Hofstetter, G., Concin, N., Fiegl, H., Müller-Holzner, E., Marth, C., Altevogt, P., and Zeimet, A. G. (2011) Regulation of transcription factor E2F3a and its clinical relevance in ovarian cancer. *Oncogene* **30,** 4038–4049 CrossRef Medline
47. Aslanian, A., Iaquinta, P. J., Verona, R., and Lees, J. A. (2004) Repression of the Arf tumor suppressor by E2F3 is required for normal cell cycle kinetics. *Genes Dev.* **18,** 1413–1422 CrossRef Medline
48. Goldschneider, D., Blanc, E., Raguenez, G., Haddada, H., Bénard, J., and Douc-Rasy, S. (2003) When p53 needs p73 to be functional: forced p73 expression induces nuclear accumulation of endogenous p53 protein. *Cancer Lett.* **197,** 99–103 CrossRef Medline
49. Miller, F. D., Pozniak, C. D., and Walsh, G. S. (2000) Neuronal life and death: an essential role for the p53 family. *Cell Death Differ.* **7,** 880–888 CrossRef Medline
50. Klein, A., Maldonado, C., Vargas, L. M., Gonzalez, M., Robledo, F., Perez de Arce, K., Muñoz, F. J., Hetz, C., Alvarez, A. R., and Zanlungo, S. (2011) Oxidative stress activates the c-Abl/p73 proapoptotic pathway in Niemann-Pick type C neurons. *Neurobiol. Dis.* **41,** 209–218 CrossRef Medline

51. Shi, B., Raina, J., Lorenzo, A., Busciglio, J., and Gabuzda, D. (1998) Neuronal apoptosis induced by HIV-1 Tat protein and TNF-α: potentiation of neurotoxicity mediated by oxidative stress and implications for HIV-1 dementia. *J. Neurovirol.* **4,** 281–290 CrossRef Medline
52. Amini, S., Mameli, G., Del Valle, L., Skowronska, A., Reiss, K., Gelman, B. B., White, M. K., Khalili, K., and Sawaya, B. E. (2005) p73 interacts with human immunodeficiency virus type 1 Tat in astrocytic cells and prevents its acetylation on lysine 28. *Mol. Cell. Biol.* **25,** 8126–8138 CrossRef Medline
53. Adams, P. D. (2007) Remodeling of chromatin structure in senescent cells and its potential impact on tumor suppression and aging. *Gene* **397,** 84–93 CrossRef Medline
54. Webber, C. A., Salame, J., Luu, G. L., Acharjee, S., Ruangkittisakul, A., Martinez, J. A., Jalali, H., Watts, R., Ballanyi, K., Guo, G. F., Zochodne, D. W., and Power, C. (2013) Nerve growth factor acts through the TrkA receptor to protect sensory neurons from the damaging effects of the HIV-1 viral protein, Vpr. *Neuroscience* **252,** 512–525 CrossRef Medline
55. Sayas, C. L., Moreno-Flores, M. T., Avila, J., and Wandosell, F. (1999) The neurite retraction induced by lysophosphatidic acid increases Alzheimer's disease-like Tau phosphorylation. *J. Biol. Chem.* **274,** 37046–37052 CrossRef Medline
56. Sun, Y., Kim, N.-H., Yang, H., Kim, S.-H., and Huh, S.-O. (2011) Lysophosphatidic acid induces neurite retraction in differentiated neuroblastoma cells via GSK-3 β activation. *Mol. Cells* **31,** 483–489 CrossRef Medline
57. Kuhla, B., Lüth, H. J., Haferburg, D., Weick, M., Reichenbach, A., Arendt, T., and Münch, G. (2006) Pathological effects of glyoxalase I inhibition in SH-SY5Y neuroblastoma cells. *J. Neurosci. Res.* **83,** 1591–1600 CrossRef Medline
58. Leuba, G., Walzer, C., Vernay, A., Carnal, B., Kraftsik, R., Piotton, F., Marin, P., Bouras, C., and Savioz, A. (2008) Postsynaptic density protein PSD-95 expression in Alzheimer's disease and okadaic acid induced neuritic retraction. *Neurobiol. Dis.* **30,** 408–419 CrossRef Medline
59. Plowey, E. D., Cherra, S. J., 3rd, Liu, Y.-J., and Chu, C. T. (2008) Role of autophagy in G2019S-LRRK2-associated neurite shortening in differentiated SH-SY5Y cells. *J. Neurochem.* **105,** 1048–1056 CrossRef Medline
60. Woronowicz, A., Amith, S. R., Davis, V. W., Jayanth, P., De Vusser, K., Laroy, W., Contreras, R., Meakin, S. O., and Szewczuk, M. R. (2007) Trypanosome trans-sialidase mediates neuroprotection against oxidative stress, serum/glucose deprivation, and hypoxia-induced neurite retraction in Trk-expressing PC12 cells. *Glycobiology* **17,** 725–734 CrossRef Medline
61. O'Dell, R. S., Cameron, D. A., Zipfel, W. R., and Olson, E. C. (2015) Reelin prevents apical neurite retraction during terminal translocation and dendrite initiation. *J. Neurosci.* **35,** 10659–10674 CrossRef Medline
62. Hoe, H.-S., Lee, K. J., Carney, R. S. E., Lee, J., Markova, A., Lee, J.-Y., Howell, B. W., Hyman, B. T., Pak, D. T.-S., Bu, G., and Rebeck, G. W. (2009) Interaction of Reelin with APP promotes neurite outgrowth. *J. Neurosci.* **29,** 7459–7473 CrossRef Medline
63. Koleske, A. J. (2013) Molecular mechanisms of dendrite stability. *Nat. Rev. Neurosci.* **14,** 536–550 CrossRef Medline
64. Niethammer, M., Smith, D. S., Ayala, R., Peng, J. M., Ko, J., Lee, M. S., Morabito, M., and Tsai, L. H. (2000) NUDEL is a novel Cdk5 substrate that associates with LIS1 and cytoplasmic dynein. *Neuron* **28,** 697–711 CrossRef Medline
65. Ovcharenko, I., Nobrega, M. A., Loots, G. G., and Stubbs, L. (2004) ECR Browser: a tool for visualizing and accessing data from comparisons of multiple vertebrate genomes. *Nucleic Acids Res.* **32,** W280–W286 CrossRef Medline